Article

pubs.acs.org/Biomac

Binding of Bacteria to Poly(*N*-isopropylacrylamide) Modified with Vancomycin: Comparison of Behavior of Linear and Highly Branched Polymers

Pavintorn Teratanatorn,[†] Richard Hoskins,[‡] Thomas Swift,[‡] C. W. Ian Douglas,[†] Joanna Shepherd,[†] and Stephen Rimmer*[,‡]

[†]Dental School, University of Sheffield, 19 Claremont Crescent, Sheffield, South Yorkshire, U.K., S10 2TA

[‡]School of Chemistry and Biosciences, University of Bradford, Bradford, West Yorkshire, U.K., BD1 1DP

Supporting Information

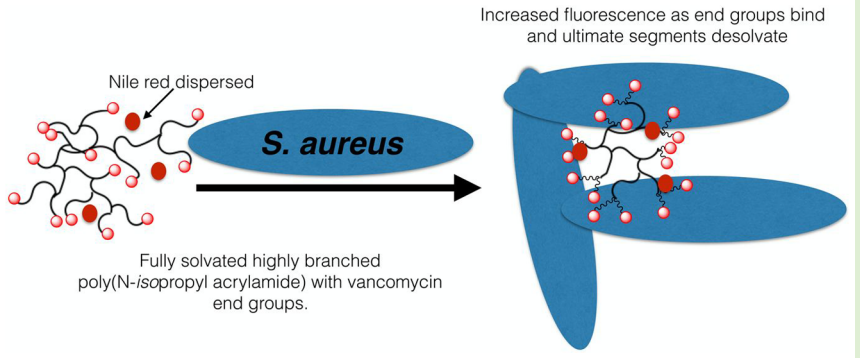

ABSTRACT: The behavior of a linear copolymer of *N*-isopropylacrylamide with pendant vancomycin functionality was compared to an analogous highly branched copolymer with vancomycin functionality at the chain ends. Highly branched poly(*N*-isopropylacrylamide) modified with vancomycin (HB-PNIPAM-van) was synthesized by functionalization of the HB-PNIPAM, prepared using reversible addition−fragmentation chain transfer polymerization. Linear PNIPAM with pendant vancomycin functionality (L-PNIPAM-van) was synthesized by functionalization of poly(*N*-isopropylacrylamide-*co*-vinyl benzoic acid). HB-PNIPAM-van aggregated *S. aureus* effectively, whereas the L-PNIPAM-van polymer did not. It was found that when the HB-PNIPAM-van was incubated with *S. aureus* the resultant phase transition provided an increase in the intensity of fluorescence of a solvatochromic dye, nile red, added to the system. In contrast, a significantly lower increase in fluorescence intensity was obtained when L-PNIPAM-van was incubated with *S. aureus*. These data showed that the degree of desolvation of HB-PNIPAM-van was much greater than the desolvation of the linear version. Using microcalorimetry, it was shown that there were no significant differences in the affinities of the polymer ligands for D-Ala-D-Ala and therefore differences in the interactions with bacteria were associated with changes in the probability of access of the polymer bound ligands to the D-Ala-D-Ala dipeptide. The data support the hypothesis that generation of polymer systems that respond to cellular targets, for applications such as cell targeting, detection of pathogens etc., requires the use of branched polymers with ligands situated at the chain ends.

INTRODUCTION

The development of simple to use devices for identification of pathogenic bacteria is an important goal in the global efforts to minimize the use of antibiotics.[1−3] Early detection of pathogens is critical in all areas of treatment of infective diseases, and recent reviews have been published that address the following: wound management,[4] urology,[5] tuberculosis,[6] blood-based infections,[7] food production,[8−10] and the supply of drinking water.[11] A number of approaches to such devices are possible, and we have introduced the idea that stimulus responsive polymers, based on poly(*N*-isopropylacrylamide) (PNIPAM), could be designed to respond to the presence of bacteria.[12−14] Several other possibilities are under investigation, including DNA based biosensors,[15,16] the use of fluorescently labeled lysozyme,[17] antibodies fabricated into microfluidic devices,[18] agglutination of nanoparticles,[19] the use of paper based devices,[20] and the measurement of the autofluorescence of infecting bacteria.[21] Another approach involves detection of bacteria derived metabolites as they adsorb to gold nanoparticles.[22] However, developing systems for the point-of care use is difficult because many of the new approaches require laboratory-based instrumentation.[23]

PNIPAM is a thermally responsive polymer that has generated considerable interest. In aqueous media, PNIPAM

Received: June 8, 2017
Revised: July 19, 2017
Published: July 21, 2017

DOI: 10.1021/acs.biomac.7b00800
Biomacromolecules XXXX, XXX, XXX−XXX

passes through a coil-to-globule transition, as chain segments become desolvated cooperatively, at a lower critical solution temperature (LCST).[24,25] These polymers and related copolymers have a number of potentially useful biological applications,[26−31] and recently, highly branched PNIPAM (HB-PNIPAM) was modified in order to attach it to bacteria.[12−14] HB-PNIPAM with bacteria binding end groups, targeted at either Gram-positive or Gram-negative species, produced aggregates of polymer and bacteria both above and below the (nonbound) LCST. However, cooling the mixtures broke up the aggregates. Following these observations, it was later shown, using Förster energy transfer with labeled polymers, that the polymers were driven through a coil-to-globule transition on binding.[32]

As our work advanced in this area, a hypothesis was developed as follows: that highly branched polymers can be driven through a coil-to-globule transition in aqueous media when the end groups are bound to targets but linear polymers with pendant ligands dissociate as the ligand−target interactions become shielded by the polymer in a transient globular state. However, until now, we have not directly compared the behavior of HB-PNIPAM with vancomycin end groups (HB-PNIPAM-van) to analogous linear PNIPAM with pendant vancomycin (L-PNIPAM-van).

Many studies on the adhesion of bacteria to nonfunctionalized polymer surfaces are available usually with a view to minimizing the adhesion of bacteria. Polymer brushes with hydrophilic or zwitterionic polymer arms are known to minimize adhesion.[33−36] These interfaces are thought to be nonfouling because adhesion of bacteria involves a reduction in the entropy of the polymer arms. The same concept can be applied to highly branched polymers, which in common with brushes present many segments with many free chain ends to bacteria as they interact with the interface. Therefore, one should expect that following adsorption of bacteria to an interface of highly branched polymers the interface would lose entropy as the bacteria adsorbs so that adsorption would become unfavorable. Both hydrophobicity and roughness are also known to affect the adhesion of bacteria,[37] and we showed that outer membrane protein A of *Escherichia coli* can have a role as bacteria interact with various hydrogel interfaces.[38] However, only a few reports are concerned with adhesion of bacteria that is dominated by the interactions with polymer bound ligands on surfaces.[39] In addition to our work on highly branched polymers with peptide end groups, others have studied polymers with pendant groups that bind bacterial lectins.[36,40−42]

Recently, Plenderleith et al. showed that nile red could be used for probing the solvation state of PNIPAM with varying degrees of branching and at varying temperatures.[43] In that work, it was shown using calorimetry that the amount of water involved in the temperature driven desolvation (coil-to-globule transition) was reduced as the degree of branching increased. When nile red was dissolved in a range of solvents, the fluorescence emission spectra of nile red changed, shifting to lower wavelength as the solvent polarity decreased. Similarly, in aqueous solutions of the HB-PNIPAMs and nile red, the wavelength of the maximum emission intensity decreased at the LCST. Therefore, in this work, this dye has been used as a fluorescent probe, to investigate differences in behavior between a HB-PNIPAM with vancomycin end groups and an analogous linear polymer with pendant vancomycin functionality. Nile red (9-diethylamino-5*H*-benzophenoxazine-5-one) is a solvatochromic uncharged hydrophobe, and the color and fluorescence change with the polarity of the environment. In nonpolar solvents, it fluoresces with a high quantum yield at an emission maximum of about 530 nm, whereas the fluorescence is decreased significantly in water.[44]

In this study, we used a range of techniques to compare linear functionalized vancomycin polymer (L-PNIPAM-van) to highly branched vancomycin polymer (HB-PNIPAM-van). For clarity, in our work, we differentiate between branched polymers with branches attached to single branch points (such as combs or graft copolymers) and polymers with branches-on-branches by referring to the latter as highly branched polymers. The linear PNIPAM was carefully formulated such that the polymer contained the same amount of vancomycin and the same fraction of repeat units containing aryl groups. This latter aspect was required because the HB-PNIPAM contains aryl branch points and this was designed into the linear polymer by copolymerization of NIPAM with vinyl benzoic acid. The data reveal important differences between the behavior of the two chemically equivalent but architecturally different polymers in their interactions with *S. aureus*.

MATERIALS AND METHODS

Materials. *N*-Isopropylacrylamide (NIPAM) (Sigma-Aldrich, 97%) was recrystallized three times from *n*-hexane/toluene (60:40). Vinyl benzoic acid (Sigma-Aldrich, 97%) was used as received. 1,4-Dioxane (Analarnormapur), *N*,*N*-dimethylformaldehyde (DMF) (Analarnormapur), and diethyl ether (Analarnormapur) were obtained from VWR and used as purchased. 4,4-Azobis(4-cyanovaleic acid) (Alfaraeser, 98%), *N*-hydroxysuccinimide (98%), *N*,*N*-dicyclohexylcarbodiimide (98%), vancomycin-hydrochloride, nile red (Sigma-Aldrich, %), toluene, and ethyl acetate were all obtained from Sigma-Aldrich and used as received. Phosphate buffer tablets (pH 7.4) and dimethyl sulfoxide (DMSO > 99.9%) were obtained from Sigma-Aldrich. Mouse monoclonal and rabbit polyclonal antibodies to vancomycin and goat antirabbit IgG conjugated to horse radish peroxidase (HRP) were obtained from Abcam Plc (Cambridge, U.K.) and diluted for use as shown below. Vinylbenzyl-pyrrolecarbodithioate (**1**) used as a chain transfer agent was synthesized as previously described.[43]

Synthesis. *Highly Branched Pyrrole/Carboxylic Acid Terminated Polymer.* HB-PNIPAM was synthesized by polymerizing *N*-isopropylacrylamide (NIPAM) (5 g, 0.04419 mol) with 4-vinylbenzyl-1-pyrrolecarboditioate (**1**, RAFT agent) (0.435 g, 0.00177 mol) in 1,4-dioxane (30 mL) at 60 °C for 48 h. 4,4-azobis(4-cyanovaleric acid) (ACVA) (0.4704 g, 0.00177 mol) was used as an initiator in order to obtain carboxylic acid chain ends, which are available for further modification. By ^{1}H NMR, conversion of crude product was 92% before purification. The highly branched polymers were purified by reprecipitation three times from dioxane with diethyl ether. HB-PNIPAM with pyrrole end groups was converted to carboxylic acid chain ends by reacting 20 equiv of 4,4-azobis(4-cyanovaleic acid) (×3) at 60 °C in DMF. ^{1}H NMR (400 MHz, DMSO) (ppm): d 0.9−1.1 (6H, s, −N(CH_3)$_2$), d 1.3−1.7 (2H, br m, −CH_2−CH−Ar−), d 1.8−2.5 (2H, br m, −CH_2−CH−CO−NH−) and (1H br m, CH_2−CH−CONH−), d 3.8 (1H br s, (CH_3)$_2$CH−), d 6.4 (H2, Br s, N−pyrrole−H), d 6.6−7.6 (br, m, −Ar−), d 7.7 (2H, br s, N−pyrrole−H). M_n = 551 kDa, M_w = 3017 kDa, M_z = 5990 kDa, $Đ_{(w/n)}$ = 5.47, $Đ_{(z/w)}$ = 1.98.

Synthesis of HB-PNIPAM Modified with Vancomycin (HB-PNIPAM-van). HB-PNIPAM-COOH (1 g) was dissolved in DMF (10 cm^3). *N*-Hydroxysuccinimide (NHS) (0.1636 g, 0.00142 mol) and *N*,*N*-dicyclohexylcarbodiimide (DCC) (0.2930 g, 0.00142 mol) were dissolved in DMF (5 cm^3) and then added to HB-PNIPAM-COOH in DMF solution. The reaction was conducted under an atmosphere of nitrogen overnight. DMF was removed by rotary evaporation, and the product was precipitated in diethyl ether. The resultant solid (HB-

DOI: 10.1021/acs.biomac.7b00800
Biomacromolecules XXXX, XXX, XXX−XXX

PNIPAM-succinimide) was purified by ultrafiltration three times in acetone:ethanol (9:1). Then, the solvent was removed by rotary evaporation and the polymer dried under a vacuum at room temperature. ^{1}H NMR (400 MHz, DMSO) (ppm): d 0.9−1.1 (6H, s, −N(CH_3)$_2$), d 1.3−1.7 (2H, br m, −CH_2−CH−Ar−), d 1.8−2.5 (2H, br m, −CH_2−CH−CO−NH−) and (1H br m, CH_2−CH−CONH−), d 3.8 (1H br s, (CH_3)$_2$CH−), d 6.4 (H2, Br s, N−pyrrole−H), d 6.6−7.6 (br, m, −Ar−), d 8.0 (1H, br s, N−pyrrole−H), d 12.0 (br m, COOH). M_n = 226 kDa, M_w = 3941 kDa, M_z = 7400 kDa, $Đ_{(w/n)}$ = 17.4, $Đ_{(z/w)}$ = 1.87.

HB-PNIPAM-succinimide (100 mg) was dissolved in deionized water (5 cm^3) over ice, and then, vancomycin (30 mg, 0.0207 mmol) dissolved in deionized water (2 mL) and phosphate buffer (2 mL) were added. The pH was adjusted with sodium hydroxide (0.1 mol dm^{-3}) to obtain a final pH of 9.5. The solution was stirred over ice for 24 h, and then, the HB-PNIPAM functionalized with vancomycin was purified by ultrafiltration three times in deionized water. The polymer was then freeze-dried and stored at −20 °C. ^{1}H NMR (400 MHz, DMSO) (ppm): d 0.9−1.1 (6H, s, −N(CH_3)$_2$), d 1.3−1.7 (2H, br m, −CH_2−CH−Ar−), d 1.8−2.2 (2H, br m, −CH_2−CH−CO−NH−) and (1H br m, CH_2−CH−CONH−), d 3.9 (1H br s, (CH_3)$_2$CH−), d 6.4 (H_2, Br s, N−pyrrole−H), d 6.6−7.6 (br, m, −Ar−), d 7.7 (2H, br s, N−pyrrole−H). M_n = 2001 kDa, M_w = 6963 kDa, M_z = 10,547 kDa, $Đ_{(w/n)}$ = 3.48, $Đ_{(z/w)}$ = 1.52.

Synthesis of Linear Poly(N-isopropylacrylamide)-co-vinyl Benzoic Acid Functionalized P(NIPAM-co-VBA). The linear analogue of the carboxylic acid terminated hyperbranched poly(*N*-isopropylacrylamide) was synthesized by copolymerizing NIPAM (5 g, 0.04419 mol) with vinyl benzoic acid (VBA) (0.249 g, 0.00168 mol) using 4,4-azobis(4-cyanovaleic acid) (0.47 g, 0.00168 mol) as an initiator in 1,4-dioxane (30 mL) at 60 °C in order to obtain the same amount of carboxylic groups along the main chain as the highly branched polymers. ^{1}H NMR (400 MHz, DMSO) (ppm): d 0.9−1.1 (6H, s, −N(CH_3)$_2$), d 1.3−1.7 (2H, br m, −CH_2−CH−Ar−), d 1.8−2.2 (2H, br m, −CH_2−CH−CO−NH−) and (1H, br m, CH_2−CH−COONH−), d 3.9 (1H, br s, (CH_3)$_2$CH−), d 6.4 (H_2, br s, N−pyrrole−H), d 6.6−7.6 (br m, −Ar−), d 12.2 (br m COOH). M_n = 554 kDa, M_w = 661 kDa, M_z = 730 kDa, $Đ_{(w/n)}$ = 1.19, $Đ_{(z/w)}$ = 1.10.

Synthesis of Linear Poly(N-isopropylacrylamide)-Functionalized with Vancomycin (L-PNIPAM-van). P(NIPAM-*co*-VBA) (100 mg) was dissolved in deionized water (5 cm_3) over ice, and then, vancomycin (30 mg, 0.0207 mmol) dissolved in deionized water (2 mL) and phosphate buffer (2 mL) were added. The pH was adjusted with sodium hydroxide (0.1 M) to obtain a final pH of 9.5. The solution was stirred over ice for 24 h, and then, the HB-PNIPAM functionalized with vancomycin was purified by ultrafiltration three times in deionized water. The polymer was then freeze-dried and stored at −20 °C. ^{1}H NMR (400 MHz, D_2O) (ppm): d 0.9−1.1 (6H, s, −N(CH_3)$_2$), d 1.3−1.7 (2H, br m, −CH_2−CH−Ar−), d 1.8−2.2 (2H, br m, −CH_2−CH−CO−NH−) and (1H, br m, CH_2−CH−COONH−), d 3.9 (1H, br s, (CH_3)$_2$CH−), d 6.4 (H2, br s, N−pyrrole−H), d 6.6−7.6 (br m, −Ar−). M_n = 637 kDa, M_w = 847 kDa, M_z = 989 kDa, $Đ_{(w/n)}$ = 1.33, $Đ_{(z/w)}$ = 1.16.

Polymer Characterization. *^{1}H NMR Spectroscopy.* All ^{1}H NMR spectra were measured and recorded on a Bruker Avance 400 NMR spectrometer running at 400 MHz.

FTIR. FT-IR measurements were carried out on a Thermo Scientific Nicolet iS10 FT-IR spectrometer. Solid samples were dried in a vacuum oven overnight before use.

Size Exclusion Chromatography (SEC). The average molar masses of the polymers were determined by GPC by elution with methanol.[45] Samples were dissolved at 1 mg mL^{-1} and injected through three Agilent Polargel-M columns at 1 mL min^{-1} flow rate, maintained at a constant 30 °C. They were analyzed via comparison to a universal calibration using PNIPAM standards via triple RI, UV, and viscometric detection to give absolute molar mass averages and dispersity ($Đ_{w/n}$ = M_w/M_n and $Đ_{z/w}$ = M_z/M_w).

Determination of LCST.

a. Micro differential scanning calorimetry (microDSC) was conducted using a VP-DSC microcalorimeter. The lower critical solution temperature (LCST) in polymer solution (1 mg cm^{-3}) was defined as the temperature corresponding to the peak of the thermogram. The samples were degassed using ThermoVac and heated and cooled from 10 to 45 °C, with a heating rate of 0.5 °C min^{-1}. The vancomycin modified polymer concentration was 10 mg cm^{-3}.
b. Turbimetry was used to measure the cloud point of polymers using a Cary 300 bio UV−visible spectrophotometer. The cloud point was determined at 550 nm over a range of temperatures from 10 to 70 °C. The samples were prepared in deionized water at a concentration of 1 mg mL^{-1}. The heating rate was 1 °C min^{-1}. The onset temperature was defined as the first stage of the onset of turbidity. In the case of vancomycin derivative polymers, the concentration was 10 mg cm^{-3}.

Confocal Microscopy. Bacteria−polymer complexes were viewed by confocal microscopy using *S. aureus* that were labeled with the fluorescent dye, Alexa Fluoro 488 (NHS).

Fluorescence Measurements. The fluorescence intensity of nile red added to the polymer−bacteria mixtures was measured in a microplate reader (Tecan Spectrophotometer, infinite M200) using 550 nm_{ext} and 600−700 nm_{emm}. The results were analyzed via Tecan Magellan software.

Bacteria. For most experiments, the standard laboratory strain of *S. aureus* Oxford (NCTC 6571) was used as a representative Gram-positive, skin wound pathogen. Bacteria were maintained on brain heart infusion agar (BHI agar), and for use, bacteria were incubated in BHI broth at 37 °C overnight, washed, and resuspended in PBS to obtain the desired concentration (cfu mL^{-1}) of bacteria.

Pseudomonas aeruginosa was used as an exemplar Gram-negative species. *P. aeruginosa* was prepared as described for *S. aureus*.

Aggregation Assay. The ability of the highly branched and linear vancomycin-functionalized polymers to bind *S. aureus* and *P. aeruginosa* was assessed by an aggregation assay. The bacteria were fluorescently labeled with Alexa Fluoro 488 (NHS). Alexa Fluoro 488 (NHS) dye stock solution was prepared in DMSO (1 mg cm^{-3}) and diluted to 1:10 in PBS before adding to bacteria (10^8 cfu mL^{-1}) resuspended in bicarbonate buffer, pH 8.6. Samples were dispersed at 4 °C with shaking in the dark for 1 h. Bacteria were then washed by centrifugation exhaustively to remove unbound dye.

The resultant fluorescently labeled bacteria were added to polymer solutions (5 mg mL^{-1}) in PBS at 37 °C in round-bottomed 96-well plates. Plates were inspected after 2, 4, and 24 h. Separate solutions of HB-PNIPAM-van and L-PNIPAM-van alone and suspensions of *S. aureus* and *P. aeruginosa* alone in PBS under the same conditions acted as controls. Samples were viewed under UV light, and parallel samples were viewed by confocal microscopy.

Peptide Interaction. Vancomycin-functionalized polymer solution (1 mL) in PBS (5 mg mL^{-1}) was mixed with varying amounts of *N*-acetyl-D-Ala-D-Ala peptide in PBS (1 mg mL^{-1} stock solution). Mixed solutions were incubated for 10 min at room temperature before microDSC was conducted using VP-DSC and the LCST determined as described above.

Addition of Nile Red to Polymer Incubated with Bacteria. To explore the solvation state of the polymers, the solvatochromic dye, nile red, was added to polymer−bacteria mixtures. All polymer samples and suspensions of bacteria were prepared as previously described. However, for the incubation steps, the polymers were incubated with *S. aureus* in flat 96-well plates to measure fluorescence intensity. After 2 h of incubation, nile red solution (0.03 mg/cm^3) in PBS (100 μL) was added directly to all samples and the fluorescence intensity was measured using a micro plate reader with Tecan Magellan software. The excitation wavelength was 550 nm. The fluorescence intensity of samples was measured after 4 and 24 h of incubation.

Quantification of Vancomycin in Polymers. A sandwich-enzyme-linked immunosorbent assay (ELISA) was used to determine the quantities of vancomycin in the highly branched and linear functionalized polymers. Flat bottomed ELISA 96-well plates (Microlon, high binding Grenier bio-one) were coated with mouse antivancomycin monoclonal antibody diluted 1/500 in carbonate

DOI: 10.1021/acs.biomac.7b00800
Biomacromolecules XXXX, XXX, XXX−XXX

Scheme 1. Synthesis of L-PNIPAM-van

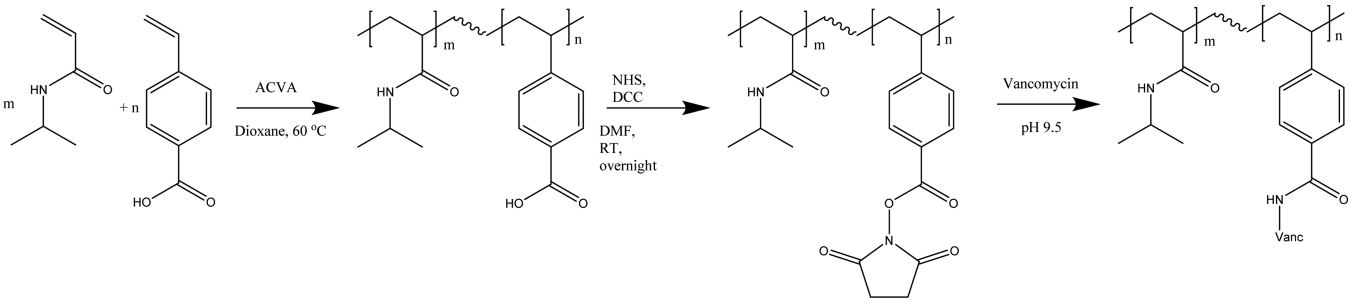

Scheme 2. Synthesis of HB-PNIPAM-van

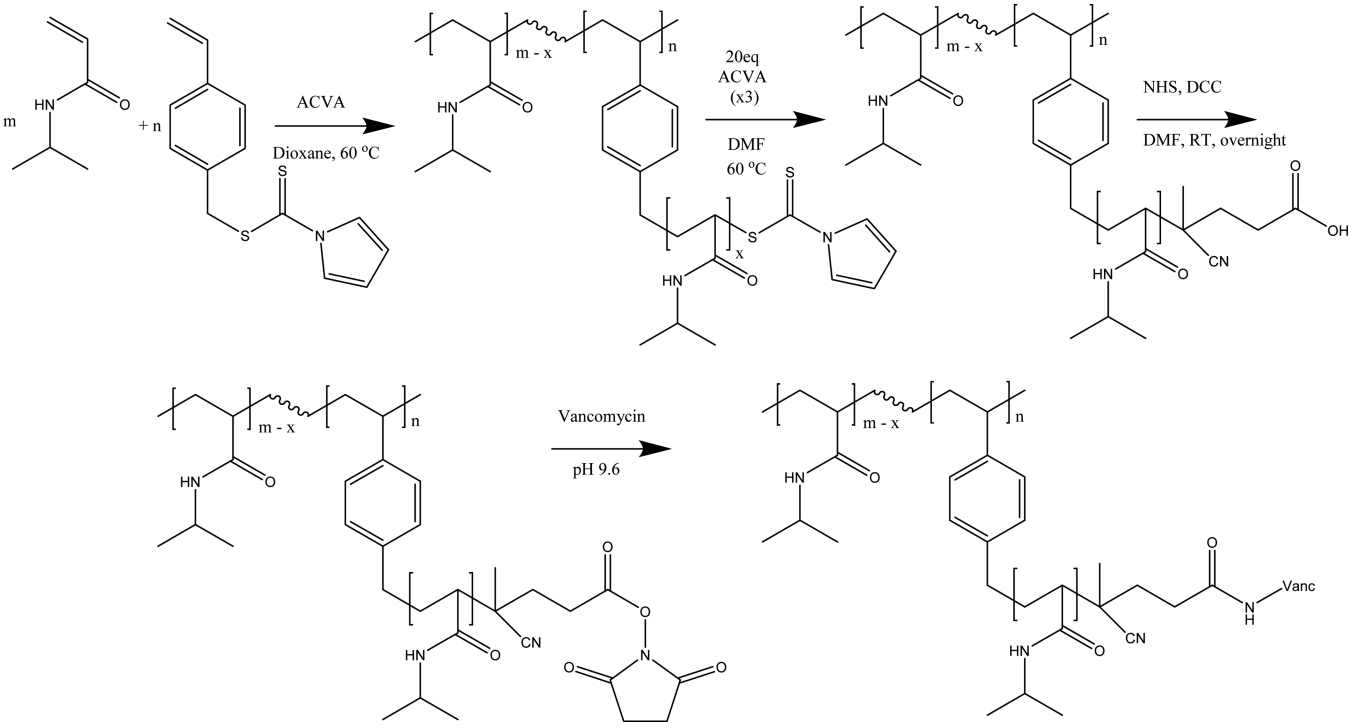

Table 1. Characterization Data for HB-PNIPAM-van and L-PNIPAM-van

polymer	M_n (kg mol^{-1})	M_w (kg mol^{-1})	Đ	*B*-ratio[a]	*α*	Vanc[b]
HB-PNIPAM-van	2001	6963	3.48	0.046	0.31	0.025
L-PNIPAM-van	637.2	847.7	1.33	0.043	0.68	0.028

[a]Ratio of benzyl groups:NIPAM from ^{1}H NMR. [b]mg mL^{-1} loading of Vanc (per mg of polymer).

buffer pH 9.6 at 4 °C overnight. After washing with PBS-tween (0.05% v/v tween) four times to remove unbound antibody, wells were blocked with 3% (w/v) bovine serum albumin (BSA) in PBS for 1 h at 37 or 4 °C overnight in order to block unoccupied binding sites on the polystyrene. Excess blocking agent was removed by washing with PBS-tween four times, and then, polymer samples and controls (PBS blank, HB-PNIPAM-COOH) in 1% BSA/PBS were added to wells and incubated overnight at 4 °C. Wells were again washed four times with PBS-tween, and rabbit antivancomycin polyclonal diluted 1/3000 in 1% BSA/PBS was added and incubated for 2 h at room temperature followed by washing with PBS-tween four times. Finally, goat antirabbit IgG conjugated to HRP in 1% BSA/PBS was added for 1 h at room temperature. After washing, wells were developed by the addition of 3,3,5,5-tetramethylbenzidine substrate plus hydrogen peroxide (30% v/v). The reaction was stopped after 25 min by addition of 2 M H_2SO_4 and the resultant color measured at 450 nm.

RESULTS

Polymer Characterization. L-PNIPAM-van was produced from a linear copolymer of NIPAM and VBA. The pendent carboxylic acid groups were activated to give the NHS ester, and then, these were modified with vancomycin. HB-PNIPAM-van was synthesized via RAFT polymerization, and the polymer chain ends were then modified with vancomycin. Changes in M_w/M_n occurred during the different stages, which reflect some chain−chain coupling and the removal of low molar mass material during ultrafiltration. Vancomycin is an antibiotic that binds to the peptidoglycan within Gram-positive bacteria cell walls. The synthesis pathway for HB-PNIPAM-van followed our previously reported route,[13] and both synthesis routes are shown in Schemes 1 and 2. The final characterization data of

DOI: 10.1021/acs.biomac.7b00800
Biomacromolecules XXXX, XXX, XXX−XXX

the vancomycin functionalized polymers are shown in Table 1 and Figure 1.

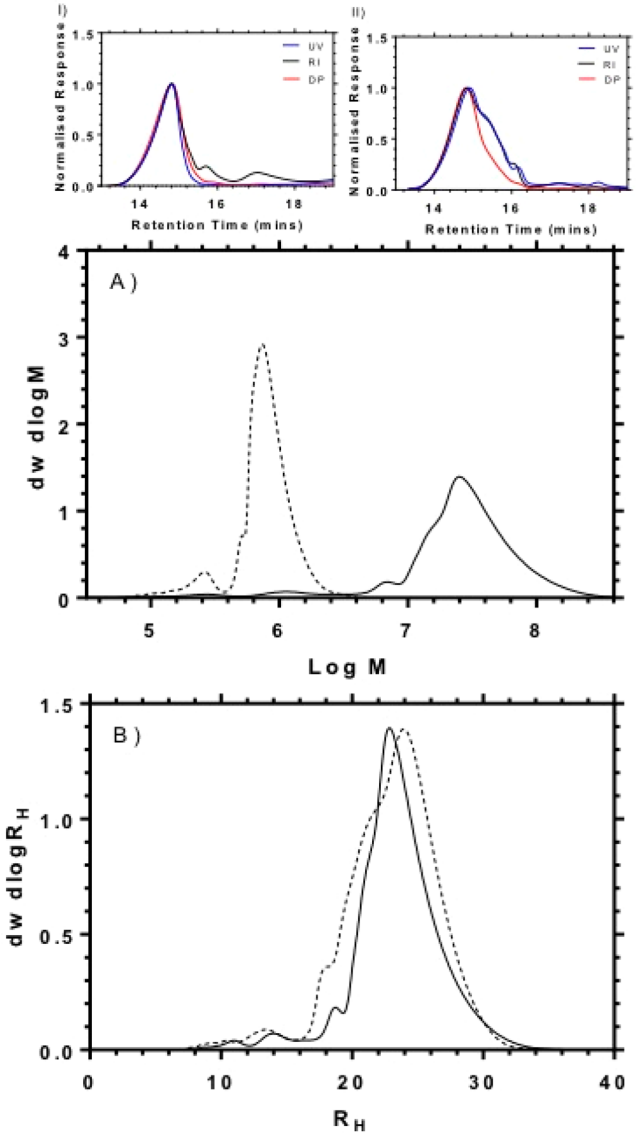

Figure 1. SEC chromatograms showing data from RI, UV, and viscometric detectors of (I) L-PNIPAM-van and (II) HB-PNIPAM-van. (A) Molar mass distribution and (B) hydrodynamic radii distributions of (---) L-PNIPAM-van and (—) HB-PNIPAM-van.

Figure 1 shows that the highly branched polymers, although they have a much greater molar mass, exhibit similar distributions of hydrodynamic radii to the linear polymers. The synthesis of the linear polymer has been optimized to achieve this result so that the effect of changing polymer architecture can be studied independently of polymer coil size.

The SEC analysis produced the molar mass averages shown in Table 1. As shown in Figure 1, both the L-PNIPAM-van and the HB-PNIPAM-van were high molar mass polymers ($>10^5$ g mol^{-1}). However, as expected, the SCVP process provided HB-PNIPAM-van that was of higher molar mass than the L-PNIPAM-van.

The SEC analysis allows also for the determination of α, the exponent of the Mark−Houwink−Sakarada equation. α varies between 0.5 (for a theta solvent) and 1 for linear polymers, and in good solvents, α is often ≈0.7. α relates to the space occupied by the coil. Branched polymers are more compact so that their viscosity increases less, than linear polymers, as concentration increases; i.e., α is depressed. Table 1 shows that the L-PNIPAM-van had α = 0.68, and the architecture of the HB-PNIPAM-van polymer is indicated by the much lower α = 0.31. Figure 1 also shows the chromatograms derived from the UV (295 nm), RI, and DP (differential pressure) detectors. The polymers contain aromatic chromophores, and the UV detector was used to assess the distribution of these chromophores. On the other hand, the RI detector provides a response from all polymers regardless of the presence of a chromophore. The data in Figure 1 show that both data sets can be superimposed, and this indicates that the chromophores, styryl units (branch points), and vancomycin groups were distributed evenly throughout the molar mass distributions.

As shown in Figure 2, the ^{1}H NMR spectra of the HB-PNIPAM-van and L-PNIPAM-van included the usual resonances for PNIPAM along with the resonances ascribable to aryl comonomer and vancomycin units. The signals from the hydrogen atoms of the benzene rings in the vancomycin and the styryl comonomer units were observed at δ 6−8 ppm in both HB-PNIPAM and L-PNIPAM.

Modification of the chain ends and pendant functionalities to HB-PNPAM-van and L-PNIPAM-van was investigated via infrared spectroscopy, and the data are shown in Figure 3. The presence of acid ends of HB-PNIPAM-COOH was confirmed by the increase, compared to the imidazole precursor, in the peak at 1710 cm^{-1} obtained from C═O stretching of carboxylic chain ends. Subsequently, this peak diminished after the succinimide/DCC reaction and new peaks at 1735, 1780, and 1800 cm^{-1}, derived from C═O antisymmetric stretch, symmetric stretch, and carbonyl stretch, respectively, were observed. All of these peaks were absent after the vancomycin attachment step, showing polymer chain ends were modified. Similarly, changes in the IR spectra were observed at the various steps in the linear polymer.

Quantification of the amount of vancomycin substitution in the polymers was established using an enzyme-linked immunosorbent assay (ELISA). The data are given in Table 1, and importantly, both polymers contained the same amount of vancomycin.

Critical Solution Behavior. The behavior of the polymers in solution was investigated by using microcalorimetry and turbidimetry techniques. Both techniques can be used to determine the LCST, but turbidimetry requires the polymer dispersion to aggregate into structures that can scatter light. Using microcalorimetry, the LCST was shown to increase with each step in the derivatization process, as shown in Table 2. The HB-PNIPAM-van and L-PNIPAM-van had similar LCSTs of 35 and 36 °C, respectively (see Table 2).

In addition, the cloud points of all polymers were determined by the turbidimetry technique (at 550 nm) over the temperature range from 10 to 70 °C. The cloud point of HB-PNIPAM-pyrrole showed an onset point of 25 °C. This value was increased to 28 °C when the polymer was functionalized by reaction with 4,4-azobis(4-cyanopentanoic acid) (ACVA) to obtain acid chain ends. However, vancomycin derivatized HB-PNIPAM-van did not provide a cloud point, even at elevated concentration (15 mg mL^{-1}). On the other hand, there was a clear cloud point when the solution of L-PNIPAM-van was heated.

DOI: 10.1021/acs.biomac.7b00800
Biomacromolecules XXXX, XXX, XXX−XXX

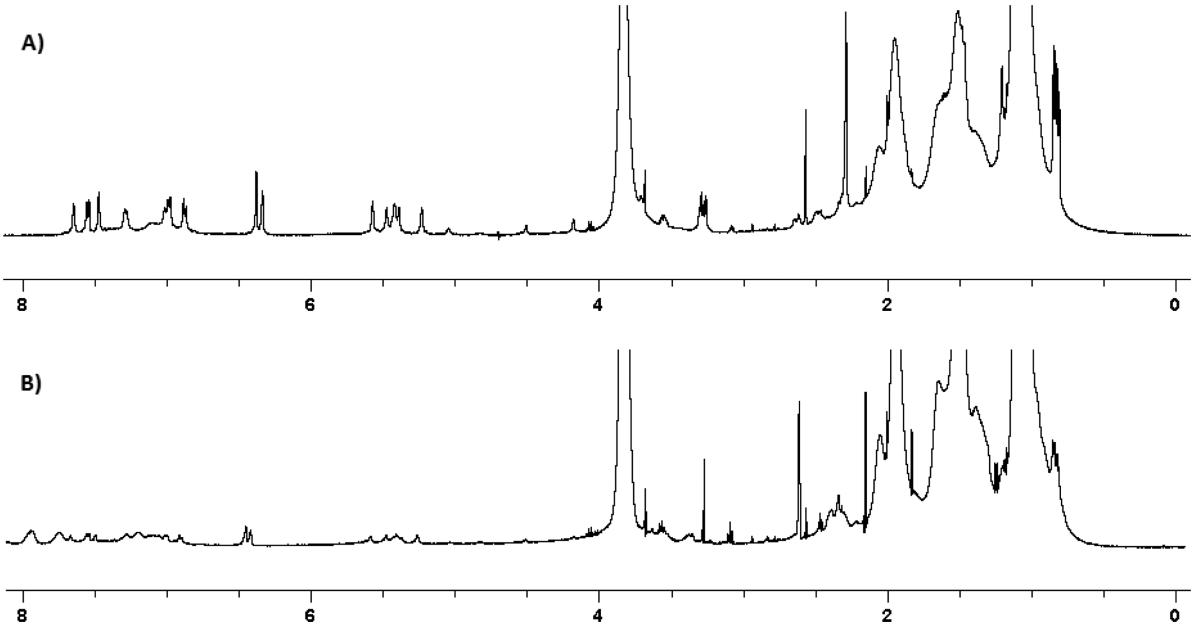

Figure 2. ^{1}H NMR of (A) HB-PNIPAM-van and (B) L-PNIPAM-van.

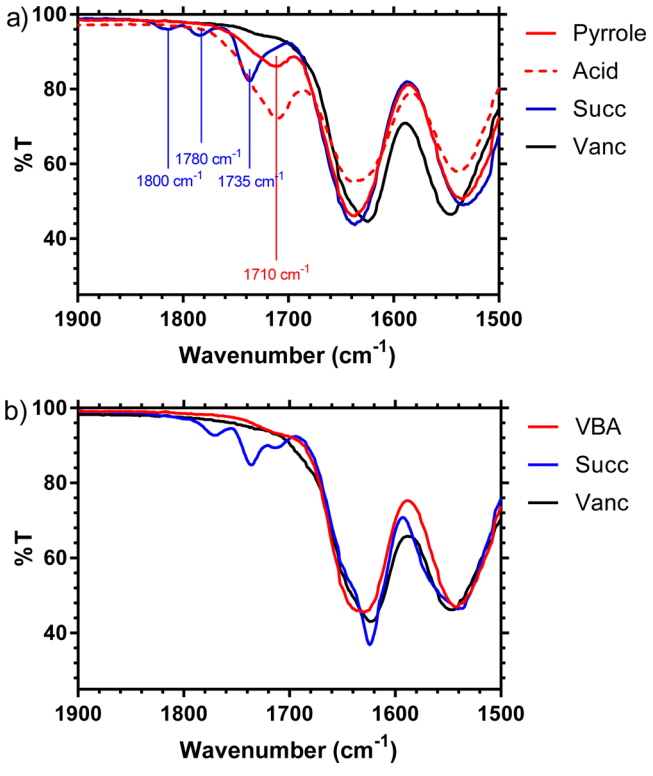

Figure 3. FTIR spectra of HB-PNIPAM (a) and linear PNIPAM (b) (1500−1900 cm^{-1}) during chain end modifications (original = red, acid modified = dashed red, succinimide modified = blue, vancomycin modified = black).

The data for the HB-PNIPAM-van show that despite the lack of a cloud point transition a LCST does occur, as indicated by the microcalorimetry data. As in the previous work,[12] a cloud point was not observed for HB-PNIPAM-van in aqueous media because the charged vancomycin groups provided electrostatic colloidal stability to the globule and this prevented aggregation.

Assessment of Polymer Binding to Bacteria. HB-PNIPAM-van and L-PNIPAM-van samples (5 mg mL^{-1}) were incubated with *S. aureus* (10^{8} cfu cm^{-3}) in PBS. The controls were *S. aureus* without polymer and HB-PNIPAM-COOH without vancomycin, and the polymers were added to a Gram-negative species, *P. aeruginosa*, which should not bind vancomycin.

Table 2. Summary of LCST Values of Linear and Highly Branched Polymers and Varying End Groups Determined by microDSC and Turbidimetry Technique

	LCST (°C)	
polymer types	microcalorimetry	turbidimetry
HB-PNIPAM	18	25
HB-PNIPAM-COOH	22	28
HB-PNIPAM-van	35	>70
L-P(NIPAM-*co*-VBA)	33	35
L-PNIPAM-van	36	39

After incubation for 24 h to allow bacteria to interact with the vancomycin-functionalized polymers, the samples were visualized by confocal microscopy and by aggregation assay. Representative images are shown in Figure 4. The bacteria were labeled with fluorophores so that they could be observed as bright spots in each panel. The data in Figure 4 show that the HB-PNIPAM-van bound to *S. aureus* (Figure 4F) producing aggregates. In contrast, no aggregates were seen with the L-PNIPAM-van (Figure 4E), which appeared similar to the controls, *S. aureus* in PBS without polymer (Figure 4D) or *S. aureus* in HB-PNIPAM-COOH. None of the vancomycin polymers produced aggregates with *P. aeruginosa*.

The images in Figure 4G−I show fluorescently labeled *S. aureus* in suspension with PNIPAM polymers in U-shape wells visualized under UV light. The bacteria appear either as a button at the bottom of the well, indicating that no aggregation has occurred (Figure 4G and H), or as a mat covering the bottom of the well, showing that aggregation has occurred (Figure 4I). Aggregation occurred with the HB-PNIPAM-van, while no aggregation occurred with the L-PNIPAM-van. Also, no aggregation occurred with L-PNIPAM-COOH or HB-PNIPAM-COOH which were control polymers that lacked

DOI: 10.1021/acs.biomac.7b00800
Biomacromolecules XXXX, XXX, XXX−XXX

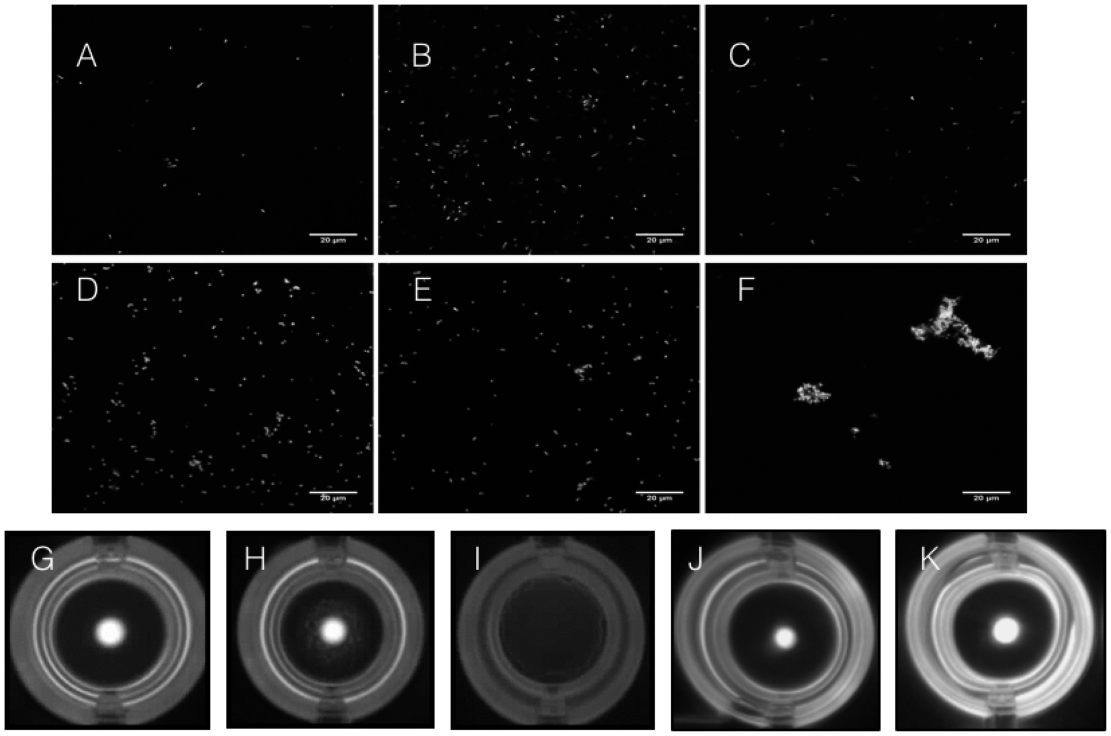

Figure 4. HB-PNIPAM-van and L-PNIPAM-van (5 mg mL^{-1}) incubated with fluorescently labeled bacteria (1×10^8 cfu mL^{-1}) for 24 h. Panels A–F show bacteria imaged by confocal microscopy, and panels G–I show aggregation assays of bacteria with polymer incubated in U-wells. *P. aeruginosa* incubated in (A) PBS alone, (B) L-PNIPAM-van in PBS, and (C) HB-PNIPAM-van in PBS. *S. aureus* incubated in (D) PBS, (E) L-PNIPAM-van in PBS, and (F) HB-PNIPAM-van in PBS. Aggregation assays of *S. aureus* (10^8 cfu mL^{-1}) in (G) PBS, (H) L-PNIPAM-van in PBS, (I) HB-PNIPAM-van in PBS, (J) L-PNIPAM-COOH, and (K) HB-PNIPAM-COOH. All were imaged under UV light. A central "button" of cells represents no aggregation, whereas a mat indicates aggregation of bacteria (I).

vancomycin (Figure 4J and K), showing that vancomycin was essential for interaction with the bacteria.

Comparison of the Interactions of HB-PNIPAM-van and L-PNIPAM-van with D-ala-D-ala Peptide. The binding target for vancomycin is the D-Ala-D-Ala peptide,[46−48] and binding prevents cell wall synthesis in Gram-positive bacteria. Therefore, to further investigate the interaction between vancomycin-functionalized PNIPAMs and Gram-positive bacteria, we examined their interaction with the D-Ala-D-Ala dipeptide using microcalorimetry and we sought to confirm that the vancomycin residues on the chain ends of the polymers were still functional and able to bind this target. In designing these experiments, we considered the hypothesis that the energy required to pass the polymer through the coil-to-globule transition would be lower when the peptide was bound than when the peptide was absent. This would be so because binding would perturb the solvation of the end groups in at least a fraction of the polymer ensemble and this fraction would be desolvated already at the observed LCST. The results of these experiments are shown in Figure 5. Control polymers (unfunctionalized HB-PNIPAM and P(NIPAM-*co*-VBA)) do not undergo a decrease in the enthalpy change at the transition on exposure to this peptide.

The data plotted in Figure 4 show the percentage enthalpy change plotted against the relative concentration of peptide (0−14 M dm^{-3}) with a fixed concentration of vancomycin attached to the polymer backbone. There was a progressive decrease in the enthalpy change when HB-PNIPAM-van was incubated with increasing concentrations of *N*-acetyl-D-Ala-D-Ala peptide. Addition of the *N*-acetyl-D-Ala-D-Ala peptide

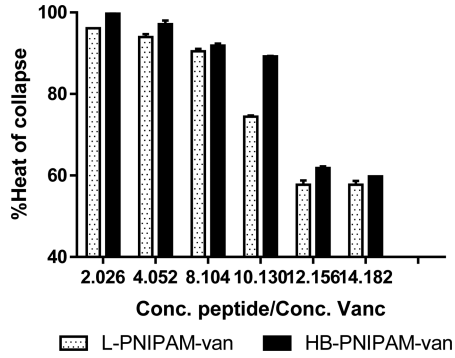

Figure 5. Changes in enthalpy as the ratio of peptide:vancomycin increased. Data shown as the fraction of the enthalpy change observed compared to in the absence of D-Ala-D-Ala.

resulted in less enthalpy change required for HB-PNIPAM-van to pass from its open to its collapsed form. The enthalpy change of HB-PNIPAM-van gradually decreased when the peptide was added from 0.347 mM dm^{-3} (75 μg) to 1.74 mM dm^{-3} (500 μg), but the enthalpy then decreased dramatically above 1.73 mM dm^{-3} (500 μg), reaching the end point at 2.08 mM dm^{-3} (600 μg) of peptide. Interestingly, the same pattern was seen with the L-PNIPAM-van; the enthalpy decreased gradually with peptide concentrations up to 1.39 mM dm^{-1} (400 μg) but then suddenly decreased, reaching a plateau at 2.42 mM dm^{-3} (700 μg). HB-PNIPAM with pyrrole chain ends and L-P(NIPAM-*co*-VBA) were used as controls and are shown in the Supporting Information.

DOI: 10.1021/acs.biomac.7b00800
Biomacromolecules XXXX, XXX, XXX−XXX

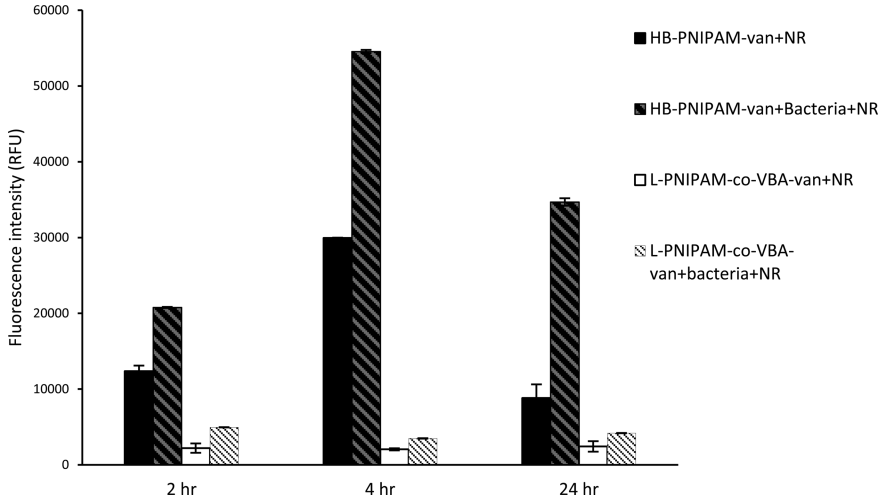

Figure 6. Relative fluorescent intensity of HB-PNIPAM-van and L-PNIPAM-van with nile red solution incubated alone and with 10^8 cfu mL^{-1} *S. aureus* (dashed) at 37 °C for 2, 4, and 24 h. λ_{ex} = 580 nm, λ_{em} = 610−680 nm.

These data indicated that as the polymers bound to the *N*-acetyl-D-Ala-D-Ala peptide sequences hydration was disrupted so that the amount of water involved was decreased, resulting in less enthalpy being consumed in the desolvation process of the polymers. Interestingly, the data showed that there was no difference between HB-PNIPAM-van and L-PNIPAM-van in the binding of the target peptide to the vancomycin sites regardless of polymer architecture.

Addition of Nile Red to HB-PNIPAM-van and L-PNIPAM-van Solutions Incubated with *S. aureus*. Since, as we reported previously,[12,32] the binding of bacteria to HB-PNIPAM-van induced a phase transition from a hydrophilic expanded state to a less solvated collapsed state, we investigated whether a solvatochromic dye could be exploited as a reporter of the solvation of the microenvironment of the polymers. The adsorption or fluorescence spectra of solvatochromic dyes such as nile red changes as the polarity of the environment changes, which can provide an indication of the solvency of the PNIPAM segments. Samples were prepared as previously described, and then, solutions of nile red in DMSO/PBS were added directly to the polymer samples and incubated with bacteria (10^8 cfu cm^{-3}) at 37 °C. The fluorescence intensity was measured after 2, 4, and 24 h, and the results shown in Figure 6 are representative of three independent experiments performed in duplicate with the fluorescence of the controls (bacteria alone) subtracted.

These results showed that the fluorescence obtained with HB-PNIPAM-van is substantially higher than that with L-PNIPAM-van. Also, at each time point, there was a substantial increase in fluorescence in the HB-PNIPAM-van system on binding to *S. aureus*. An increase in the fluorescence intensity from the L-PNIPAM-van on mixing with *S. aureus* was seen, but this was very much smaller.

Effect of the Concentration of Bacteria on the Fluorescence of Nile Red with HB-PNIPAM-van and L-PNIPAM-van. The above data were generated using a single concentration of bacteria. However, it is possible that each polymer might behave differently with varying numbers of bacteria. In this work, HB-PNIPAM-van and L-PNIPAM-van were incubated with bacteria at 10^5−10^9 cfu cm^{-3} at 37 °C for 2 h. Then, nile red solutions were added into all samples and the fluorescence intensity measured (550 nm excitation). The measurement was repeated at 4 and 24 h, and fluorescence intensities were obtained as shown in Figure 7.

From the fluorescence intensity measurement of the polymers incubated with *S. aureus* at different concentrations using nile red as a probe, it was found that at any given bacterial load the fluorescence intensity of the nile red with HB-PNIPAM-van was much greater than that seen with the L-PNIPAM-van. Furthermore, the fluorescence intensity associated with both highly branched and linear polymers decreased as the number of bacteria decreased ($10^5 < 10^6 < 10^7 < 10^8$ cfu cm^{-3}) at all incubation times. This suggests that the effect of decreasing the concentration of bacteria was to reduce the amount of polymer that passed though the phase change because fewer chain ends became bound.

DISCUSSION

Linear and branched polymers were prepared with similar chemical compositions and with equivalent degrees of vancomycin functionality. Analysis of molar mass distributions showed that the average molar masses were higher in branched polymers and the distributions were broader. However, it was possible to design the linear polymer such that it had an equivalent distribution of the hydrodynamic radii to the final highly branched variant. Also, SEC showed that the ultrafiltration process removed a low molar mass fraction from the highly branched polymer. Due to the contraction of the coil as the degree of branching increases, it is not possible to maintain constant distributions of molar masses and hydrodynamic radii simultaneously. However, in this work, we consider that the important parameter that would potentially influence interactions with cells and bacteria is likely to be coil size (hydrodynamic radii) rather than molar mass.

Turbidimetry provided phase information at the macroscopic level, and cloud points were only observed as particles aggregated into structures that were large enough to scatter visible light; that is, a cloud point was not observed when a solution of HB-PNIPAM-van was heated. However, the LCST was observed by calorimetry, which provided information on the heat released during the dehydration process without the necessity for aggregation to occur. On the other hand, L-PNIPAM-van provided both an endothermic response in the microcalorimeter and a cloud point at similar temperatures. In

DOI: 10.1021/acs.biomac.7b00800
Biomacromolecules XXXX, XXX, XXX−XXX

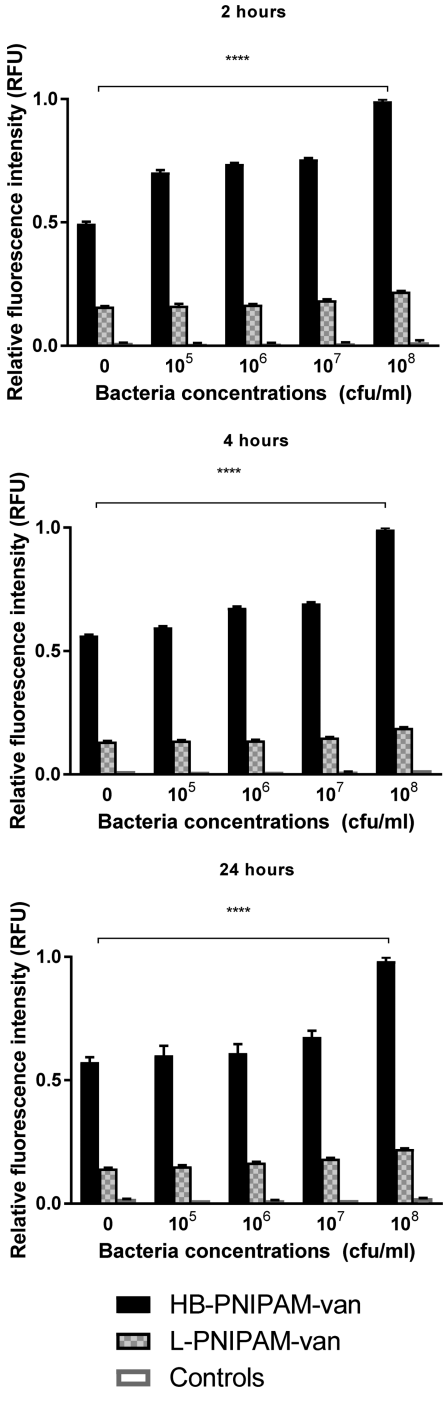

Figure 7. Fluorescent emission of nile red incubated with HB-PNIPAM-van, L-PNIPAM-van, and with no polymer (controls) at 37 °C for 2, 4, and 24 h with addition of 10^5–10^8 cfu mL^{-1} *S. aureus*.

the case of this linear polymer with pendant ligands, the coil-to-globule transition formed chain-folded structures in which the polar vancomycin pendant groups were wrapped within the globule and shielded from providing colloidal stabilization. Therefore, the coil-to-globule transition produced aggregates producing the cloud point. The lack of a cloud point from the HB-PNIPAM-van was a clear example of the change in properties observed as the polymer architecture was changed from linear to branched while the chemical composition was kept constant. Colloidal stability is enhanced because, in HB-PNIPAM, the polar (vancomycin) end groups do not penetrate the globule and remain at the surface. Thus, the HB-PNIPAM-van globules express substantial charge; they do not aggregate, and the globules are too small to scatter light.

The target for vancomycin is known to be the D-Ala-D-Ala dipeptide, and binding of this to the vancomycin end groups should perturb the solvation of the polymer. This was observed when *N*-acetyl-D-Ala-D-Ala was added to HB-PNIPAM-van in aqueous solution so that the magnitude of the endotherm at the LCST was reduced when D-Ala-D-Ala interacted with the vancomycin end groups. Interestingly, the effect of adding D-Ala-D-Ala was not to shift the peak of the transition. In our view, this decrease in the magnitude of the endotherm without a substantial change in the transition peak temperature suggests that the binding affects solvation of segments rather than the whole polymer chain. That is, binding reduced the solvation of chain end segments (located toward the outer regions of the polymer coil), but the segments distant from the chain ends remained unaffected. Desolvation of chain end segments on binding *N*-acetyl-D-Ala-D-Ala, as shown in Figure 8A, reduced the amount of water involved in desolvation at the coil-to-globule transition so that the observed endotherm was reduced. This heterogeneous desolvation is also supported by the results from adding nile red to the system, with and without bacteria. Nile red is a solvatochromic dye that preferentially can be partitioned into hydrophobic phases. In the initial experimental design, it was expected that addition of nile red to HB-PNIPAM-van would result in a solvatochromic shift (a change in the absorption spectrum) compared to addition of the dye to L-PNIPAM-van. If the binding of *S. aureus* resulted in a coil-to-globule transition, a large solvatochomic shift would be observed as a more hydrophobic polymer phase was produced. A solvatochromic shift was not observed in the presence of *S. aureus*, but there was a substantial increase in fluorescence intensity (Figure 5) of the HB-PNIPAM-van that was not observed when L-PNIPAM-van was mixed with *S. aureus*. These observations are best rationalized by considering that, in the absence of bacteria, nile red was distributed homogeneously throughout the polymer segments, but when bacteria bind and a fraction of the segments become desolvated, the nile red was partitioned between the open coil (solvated) domains and the desolvated segments. Because the system responded at the segment length scale, a large fraction would not be affected by the change of the environment of the outer segments that were bound to the bacteria. The calorimetric data also indicated that a fraction of the chain segments were not affected by binding so that it is reasonable to suggest that the major fraction of the nile red remained partitioned within open coil domains and that the minor fraction within the desolvated domains was not sufficient to produce a detectable solvatochromic shift in the adsorption spectra. On the other hand, partitioning of the nile red into the desolvated domains that are in close proximity to the bound vancomycin groups can reduce the quenching of fluorescence by reducing the exposure to the solvent and adjusting its local polarity. In our earlier work,[12] we had assumed that binding produced a general and homogeneously desolvated state, but the current data support a modified model illustrated in Figure 8. At this point, it may be instructive to consider that the calorimetric data indicate that both the HB-PNIPAM-van and the L-PNIPAM-van are in critical states at the temperature in experiments involving binding to the bacteria; i.e., the peak temperatures are 35 and 36 °C, and the temperature of the experiments was 37 °C. Figure 8A shows that in the nonbound state the polymer was solvated. Changing the temperature

DOI: 10.1021/acs.biomac.7b00800
Biomacromolecules XXXX, XXX, XXX−XXX

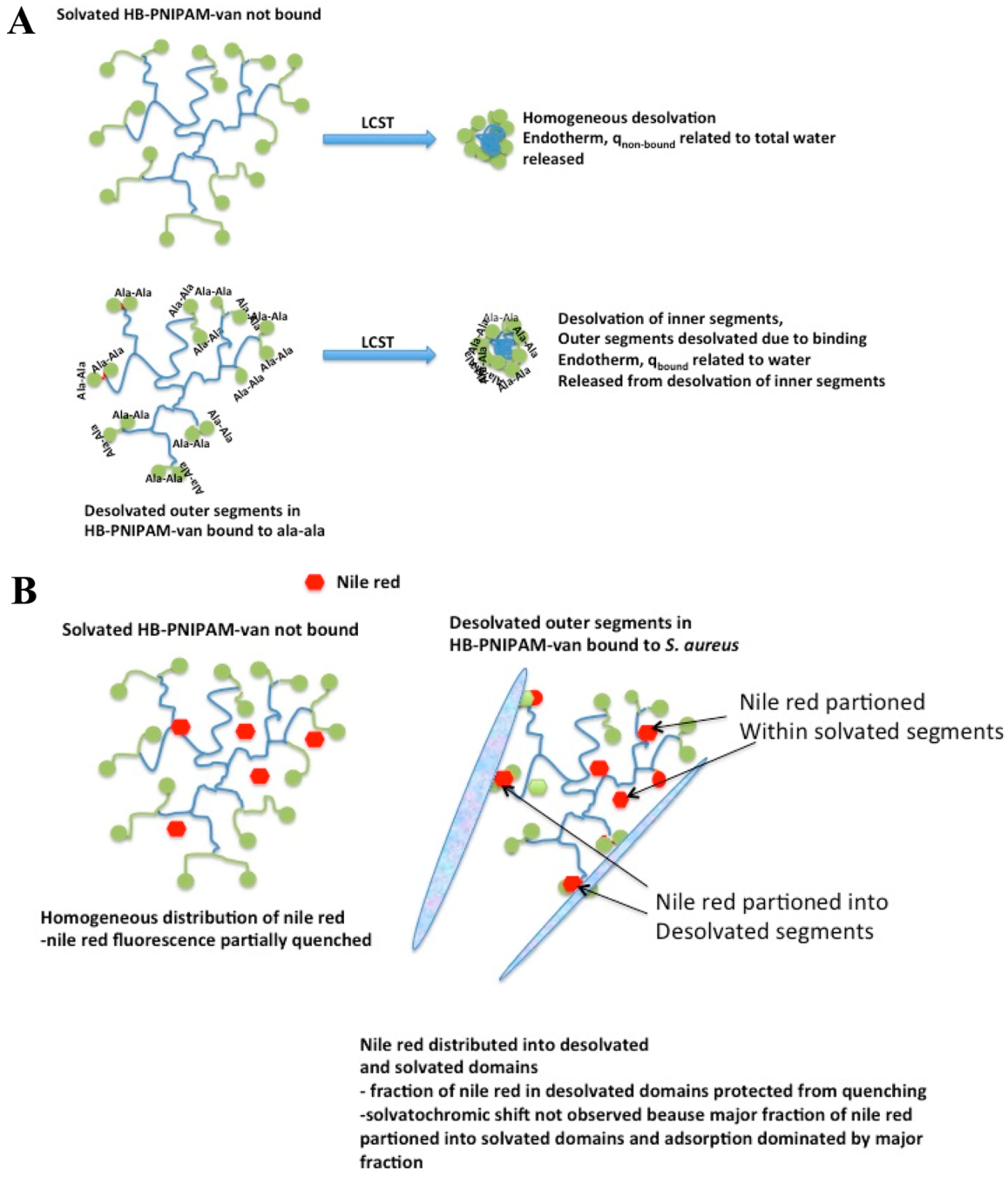

Figure 8. Nonhomogeneous response of HB-PNIPAM-van to binding. (A) The proposed response to binding of *N*-acetyl-D-Ala-D-Ala. (B) A schematic diagram showing the response to binding to bacteria (via binding to D-Ala-D-Ala).

through the LCST produced desolvation and the polymer progressed through the coil-to-globule transition, producing an endotherm due to the desolvation. The end groups are highly polar, and we consider that they partially penetrate the coil providing an osmotic pressure that swells the outer segments of the coil below the LCST.

On binding, this osmotic driven swelling is lost as the end groups become desolvated and are less polar. This results in desovation of the outer segments. Thus, when the bound form was heated and progressed though the LCST, a smaller endotherm was observed because a smaller amount of water was involved in solvation of the remaining segments. Figure 8B shows how nile red would partition in this model. In the nonbound open coil state, nile red partioned into the branched structure and quenching of fluorescence was reduced as the close proximity of the segments provided a less polar environment than the solvated linear polymer. Binding of the target provided domains in which the outer segments were desolvated, as described above, but only a fraction of the nile red became partioned into these domains. From the data, it appears that the majority of the nile red was not present in these desolvated domains so that no observable shift in the absorption spectrum was observed. However, the small fraction that was within the desolvated domains was protected from quenching and this gave rise to an increase in fluorescence.

DOI: 10.1021/acs.biomac.7b00800
Biomacromolecules XXXX, XXX, XXX−XXX

The microscopy data showed that HB-PNIPAM-van bound to these Gram-positive bacteria and formed bacteria−polymer complexes, which then formed large aggregated structures. L-PNIPAM-van did not bind to bacteria because at 37 °C the pendant vancomycin groups were shielded. Binding of the pendant vancomycin in linear polymer would be expected to provide a desolvation, but in both the globular and open coil forms, the pendant vancomycin groups were shielded by the chain segments. On the other hand, in the highly branched polymer, chain ends are predicted not to penetrate desolvated globular structures and therefore chain end vancomycin groups are available for interaction with the targets even in the desolvated state. The D-Ala-D-Ala peptide sequence lies within the peptidoglycan layer that is penetrated by lipotechoic acid (LTA) and teichoic acid that extend to varying degrees from the cell surface. The results reported here show that the isolated D-Ala-D-Ala peptide binds to vancomycin attached to either L-PNIPAM or the end groups of HB-PNIPAM. However, the behavior of *S. aureus* in the presence of the two polymers was very different. The LTA of Gram-positive bacteria ranges in thickness from just more than the peptidoglycan itself to approximately 80 nm, but on average, it is around 30 nm in thickness[49] and in the case of the L-PNIPAM it seems reasonable that shielding of the pendant vancomycin prevents access to the D-Ala-D-Ala sequences. However, the vancoycin groups at the chain ends of HB-PNIPAM are attached to terminal chain segments of on average approximately 25 repeats units. The segments will be of dimensions on the order of a few nanometers, and we propose that segments of this length can penetrate the LTA layer and access at least the outer regions of the peptide glycan domain. The shielding behavior in the linear polymers also affects colloidal stability above the LCST. Shielding behavior led to the formation of large aggregates of the L-PNIPAM-van material above the LCST. On the other hand, in the HB-PNIPAM-van globules, the vancomycin provided electrostatic colloidal stability because these groups were located at the polymer/aqueous interface. Thus, the L-PNIPAM-van did not form aggregates with *S. aureus*, but the HB-PNIPAM-van did form aggregates. Therefore, it is suggested that cross-linking and aggregation of bacteria in the presence of HB-PNIPAM-van is due not only to binding of bacteria to the vancomycin groups at the chain ends but also to the consequent phase transition, which creates a more hydrophobic-interactive environment for the bacteria.

The differences in behavior between HB-PNIPAM-van and L-PNIPAM-van were not evident when the isolated target for vancomycin was bound to the polymers, and this observation suggests that the differences in behavior in the presence of the bacteria are due to differences in the accessibility of the polymers to D-Ala-D-Ala in the cell wall. The evidence presented is consistent with the hypothesis that, above the LCST, the pendant ligands of the linear polymers became trapped inside the collapsed polymer, rendering them unavailable for binding to *S. aureus*. On the other hand, when segments of the HB-PNIPAM-van adjacent to the vancomycin ligands passed through the coil-to globule transition, the chain-end vancomycin groups did not penetrate the coil and they remained available for binding to the cellular target. The difference in behavior was clearly not due to differences in the degree of vancomycin substitution between the two forms of polymer.

CONCLUSION

Comparison of highly branched and linear analogues of PNIPAM with vancomycin end groups showed that polymer architecture plays a significant role in the performance of functional polymers after binding to targets on bacteria. The data indicated that placement of the ligands at the chain ends of branched structures is required to produce polymers that respond by passing through the coil-to-globule transition on binding to bacteria. The data indicate that binding of bacteria produces a phase transition on the segment length scale.

ASSOCIATED CONTENT

Supporting Information

The Supporting Information is available free of charge on the ACS Publications website at DOI: 10.1021/acs.biomac.7b00800.

Additional characterization data for the molar mass distribution, FTIR spectra, enthalpy of polymer collapse, raw fluorescence data, ^{1}H NMR, vancomycin structure, and photographs of nile red solutions with polymer and bacteria (PDF)

AUTHOR INFORMATION

Corresponding Author

*E-mail: S.Rimmer@Bradford.ac.uk.

ORCID

Thomas Swift: 0000-0002-8616-8458

Stephen Rimmer: 0000-0002-1048-1974

Notes

The authors declare no competing financial interest.

ACKNOWLEDGMENTS

Innovate UK and Smith and Nephew Ltd. (TSB 101224) are acknowledged for funding postdoctoral fellowships for R.H. A portion of this work was also completed by R.H. during a MRC funded project (MR/N501888/2).

REFERENCES

(1) O'Neill, J. "Rapid Diagnostics: Stopping Unnecessary Use of Antibiotics. 2015" *The Review on Antimicrobial Resistance, Wellcome Trust and HM Govement.*

(2) Ghafur, A.; Mathai, D.; Muruganathan, A.; Jayalal, J.; Kant, R.; Chaudhary, D.; Prabhash, K.; Abraham, O.; Gopalakrishnan, R.; Ramasubramanian, V.; Shah, S.; Pardeshi, R.; Huilgol, A.; Kapil, A.; Gill, J.; Singh, S.; Rissam, H.; Todi, S.; Hegde, B.; Parikh, P. *Indian J. Cancer* **2013**, *50*, 71−73.

(3) WHO, Antimicrobial Resistance, Global Report on Surveillance. *Antimicrobial Resistance, Global Report on Surveillance* 2014.

(4) Tegl, G.; Schiffer, D.; Sigl, E.; Heinzle, A.; Guebitz, G. Biomarkers for infection: enzymes, microbes, and metabolites. *Appl. Microbiol. Biotechnol.* **2015**, *99* (11), 4595−4614.

(5) Zowawi, H. M.; Harris, P. N. A.; Roberts, M. J.; Tambyah, P. A.; Schembri, M. A.; Pezzani, M. D.; Williamson, D. A.; Paterson, D. L. The emerging threat of multidrug-resistant Gram-negative bacteria in urology. *Nat. Rev. Urol.* **2015**, *12* (10), 570−584.

(6) Venturini, E.; Remaschi, G.; Berti, E.; Montagnani, C.; Galli, L.; de Martino, M.; Chiappini, E. What steps do we need to take to improve diagnosis of tuberculosis in children? *Expert Rev. Anti-Infect. Ther.* **2015**, *13* (7), 907−922.

(7) Opota, O.; Jaton, K.; Greub, G. Microbial diagnosis of bloodstream infection: towards molecular diagnosis directly from blood. *Clin. Microbiol. Infect.* **2015**, *21* (4), 323−331.

DOI: 10.1021/acs.biomac.7b00800
Biomacromolecules XXXX, XXX, XXX−XXX

(8) Josefsen, M. H.; Bhunia, A. K.; Engvall, E. O.; Fachmann, M. S. R.; Hoorfar, J. Monitoring Campylobacter in the poultry production chain — From culture to genes and beyond. *J. Microbiol. Methods* **2015**, *112*, 118−125.
(9) Rohde, A.; Hammerl, J. A.; Appel, B.; Dieckmann, R.; Al Dahouk, S. FISHing for bacteria in food − A promising tool for the reliable detection of pathogenic bacteria? *Food Microbiol.* **2015**, *46*, 395−407.
(10) Singh, J.; Sharma, S.; Nara, S. Evaluation of gold nanoparticle based lateral flow assays for diagnosis of enterobacteriaceae members in food and water. *Food Chem.* **2015**, *170*, 470−483.
(11) Mendes Silva, D.; Domingues, L. On the track for an efficient detection of Escherichia coli in water: A review on PCR-based methods. *Ecotoxicol. Environ. Saf.* **2015**, *113*, 400−411.
(12) Shepherd, J.; Sarker, P.; Swindells, K.; Douglas, I.; MacNeil, S.; Swanson, L.; Rimmer, S. Binding bacteria to highly branched poly(N-isopropyl acrylamide) modified with vancomycin induces the coil-to-globule transition. *J. Am. Chem. Soc.* **2010**, *132* (6), 1736−1737.
(13) Sarker, P.; Shepherd, J.; Swindells, K.; Douglas, I.; MacNeil, S.; Swanson, L.; Rimmer, S. Highly branched polymers with polymyxin end groups responsive to Pseudomonas aeruginosa. *Biomacromolecules* **2011**, *12* (1), 1−5.
(14) Shepherd, J.; Sarker, P.; Rimmer, S.; Swanson, L.; MacNeil, S.; Douglas, I. Hyperbranched poly(NIPAM) polymers modified with antibiotics for the reduction of bacterial burden in infected human tissue engineered skin. *Biomaterials* **2011**, *32* (1), 258−267.
(15) Singh, R.; Mukherjee, M. D.; Sumana, G.; Gupta, R. K.; Sood, S.; Malhotra, B. D. Biosensors for pathogen detection: A smart approach towards clinical diagnosis. *Sens. Actuators, B* **2014**, *197*, 385−404.
(16) Scheler, O.; Glynn, B.; Kurg, A. Nucleic acid detection technologies and marker molecules in bacterial diagnostics. *Expert Rev. Mol. Diagn.* **2014**, *14* (4), 489−500.
(17) Zheng, L.; Wan, Y.; Yu, L.; Zhang, D. Lysozyme as a recognition element for monitoring of bacterial population. *Talanta* **2016**, *146*, 299−302.
(18) Cho, S.; Park, T. S.; Nahapetian, T. G.; Yoon, J.-Y. Smartphone-based, sensitive μPAD detection of urinary tract infection and gonorrhea. *Biosens. Bioelectron.* **2015**, *74*, 601−611.
(19) Mezger, A.; Fock, J.; Antunes, P.; Østerberg, F. W.; Boisen, A.; Nilsson, M.; Hansen, M. F.; Ahlford, A.; Donolato, M. Scalable DNA-Based Magnetic Nanoparticle Agglutination Assay for Bacterial Detection in Patient Samples. *ACS Nano* **2015**, *9* (7), 7374−7382.
(20) Hu, J.; Wang, S.; Wang, L.; Li, F.; Pingguan-Murphy, B.; Lu, T. J.; Xu, F. Advances in paper-based point-of-care diagnostics. *Biosens. Bioelectron.* **2014**, *54*, 585−597.
(21) DaCosta, R. S.; Liis Lindvere-Teene, I. K.; Starr, D.; Blackmore, K.; Silver, J. I.; Opoku, J.; Charlie Wu, Y.; Medeiros, P. J.; Xu, Wei; Xu, Lizhen; Wilson, Brian C.; Linden, Cheryl RosenRon Point-of-Care Autofluorescence Imaging for Real-Time Sampling and Treatment Guidance of Bioburden in Chronic Wounds: First-in-Human Results. *PLoS One* **2015**, *10* (3), e0116623.
(22) Webster, M. S.; Cooper, J. S.; Chow, E.; Hubble, L. J.; Sosa-Pintos, A.; Wieczorek, L.; Raguse, B. Detection of bacterial metabolites for the discrimination of bacteria utilizing gold nanoparticle chemiresistor sensors. *Sens. Actuators, B* **2015**, *220*, 895−902.
(23) Pal, N.; Sharma, S.; Gupta, S. Sensitive and rapid detection of pathogenic bacteria in small volumes using impedance spectroscopy technique. *Biosens. Bioelectron.* **2016**, *77*, 270−276.
(24) Ramos, J.; Imaz, A.; Forcada, J. Temperature-sensitive nanogels: poly(N-vinylcaprolactam) versus poly(N-isopropylacrylamide). *Polym. Chem.* **2012**, *3* (4), 852−856.
(25) Grassi, G.; Farra, R.; Caliceti, P.; Guarnieri, G.; Salmaso, S.; Carenza, M.; Grassi, M. Temperature-sensitive hydrogels. *Am. J. Drug Delivery* **2005**, *3* (4), 239−251.
(26) Guan, Y.; Zhang, Y. PNIPAM microgels for biomedical applications: From dispersed particles to 3D assemblies. *Soft Matter* **2011**, *7* (14), 6375−6384.
(27) Rzaev, Z. M. O.; Dinçer, S.; Pişkin, E. Functional copolymers of N-isopropylacrylamide for bioengineering applications. *Prog. Polym. Sci.* **2007**, *32* (5), 534−595.
(28) Saunders, B. R.; Laajam, N.; Daly, E.; Teow, S.; Hu, X.; Stepto, R. Microgels: From responsive polymer colloids to biomaterials. *Adv. Colloid Interface Sci.* **2009**, *147−148* (C), 251−262.
(29) Marina Talelli, W. E. H. Thermosensitive polymeric micelles for targeted drug delivery. *Nanomedicine* **2011**, *6* (7), 1245−1255.
(30) Wei, H.; Cheng, S.-X.; Zhang, X.-Z.; Zhuo, R.-X. Thermosensitive polymeric micelles based on poly(N-isopropylacrylamide) as drug carriers. *Prog. Polym. Sci.* **2009**, *34* (9), 893−910.
(31) Cellesi, F. Thermoresponsive hydrogels for cellular delivery. *Ther. Delivery* **2012**, *3* (12), 1395−1407.
(32) Sarker, P.; Swindells, K.; Douglas, C. W. I.; MacNeil, S.; Rimmer, S.; Swanson, L. Fluorescence resonance energy transfer confirms the bacterial-induced conformational transition in highly-branched poly(N-isopropyl acrylamide with vancomycin end groups on binding to Staphylococcus aureus. *Soft Matter* **2014**, *10*, 5824−5835.
(33) Hadjesfandiari, N.; Yu, K.; Mei, Y.; Kizhakkedathu, J. N. Polymer brush-based approaches for the development of infection-resistant surfaces. *J. Mater. Chem. B* **2014**, *2* (31), 4968−4978.
(34) Salwiczek, M.; Qu, Y.; Gardiner, J.; Strugnell, R. A.; Lithgow, T.; McLean, K. M.; Thissen, H. Emerging rules for effective antimicrobial coatings. *Trends Biotechnol.* **2014**, *32* (2), 82−90.
(35) Banerjee, I.; Pangule, R. C.; Kane, R. S. Antifouling Coatings: Recent Developments in the Design of Surfaces That Prevent Fouling by Proteins, Bacteria, and Marine Organisms. *Adv. Mater. (Weinheim, Ger.)* **2011**, *23* (6), 690−718.
(36) Zhao, C.; Zheng, J. Synthesis and Characterization of Poly(N-hydroxyethylacrylamide) for Long-Term Antifouling Ability. *Biomacromolecules* **2011**, *12* (11), 4071−4079.
(37) Juvonen, H.; Oja, T.; Määttänen, A.; Sarfraz, J.; Rosqvist, E.; Riihimäki, T. A.; Toivakka, M.; Kulomaa, M.; Vuorela, P.; Fallarero, A.; Peltonen, J.; Ihalainen, P. Protein and bacterial interactions with nanostructured polymer coatings. *Colloids Surf., B* **2015**, *136*, 527−535.
(38) Orme, R.; Douglas, C. W. I.; Rimmer, S.; Webb, M. Proteomic analysis of Escherichia coli biofilms reveals the overexpression of the outer membrane protein OmpA. *Proteomics* **2006**, *6* (15), 4269−4277.
(39) Xue, Y.; Guan, Y.; Zheng, A.; Wang, H.; Xiao, H. Synthesis and Characterization of Ciprofloxacin Pendant Antibacterial Cationic Polymers. *J. Biomater. Sci., Polym. Ed.* **2012**, *23* (8), 1115−1128.
(40) Hansen, R. R.; Hinestrosa, J. P.; Shubert, K. R.; Morrell-Falvey, J. L.; Pelletier, D. A.; Messman, J. M.; Kilbey, S. M.; Lokitz, B. S.; Retterer, S. T. Lectin-Functionalized Poly(glycidyl methacrylate)-block-poly(vinyldimethyl azlactone) Surface Scaffolds for High Avidity Microbial Capture. *Biomacromolecules* **2013**, *14* (10), 3742−3748.
(41) Wang, W.; Chance, D.; Mossine, V.; Mawhinney, T. RAFT-based tri-component fluorescent glycopolymers: synthesis, characterization and application in lectin-mediated bacterial binding study. *Glycoconjugate J.* **2014**, *31* (2), 133−143.
(42) Pasparakis, G.; Cockayne, A.; Alexander, C. Control of Bacterial Aggregation by Thermoresponsive Glycopolymers. *J. Am. Chem. Soc.* **2007**, *129* (36), 11014−11015.
(43) Plenderleith, R.; Swift, T.; Rimmer, S. Highly-branched poly(N-isopropyl acrylamide)s with core-shell morphology below the lower critical solution temperature. *RSC Adv.* **2014**, *4* (92), 50932−50937.
(44) Greenspan, P.; Fowler, S. D. Spectrofluorometric studies of the lipid probe, nile red. *J. Lipid Res.* **1985**, *26* (7), 781−9.
(45) Swift, T.; Hoskins, R.; Telford, R.; Plenderleith, R.; Pownall, D.; Rimmer, S. Analysis Using Size Exclusion Chromatography of poly(N-isopropyl acrylamide) using Methanol as an Eluent. *J. Chromatogr. A* **2017**, *1508*, 16−23.
(46) Rekharsky, M.; Hesek, D.; Lee, M.; Meroueh, S. O.; Inoue, Y.; Mobashery, S. Thermodynamics of Interactions of Vancomycin and Synthetic Surrogates of Bacterial Cell Wall. *J. Am. Chem. Soc.* **2006**, *128* (24), 7736−7737.

DOI: 10.1021/acs.biomac.7b00800
Biomacromolecules XXXX, XXX, XXX−XXX

(47) Lee, J.-G.; Sagui, C.; Roland, C. First Principles Investigation of Vancomycin and Teicoplanin Binding to Bacterial Cell Wall Termini. *J. Am. Chem. Soc.* **2004**, *126* (27), 8384−8385.
(48) Carpenter, J. L.; Camilleri, P.; Dhanak, D.; Goodall, D. A study of the binding of vancomycin to dipeptides using capillary electrophoresis. *J. Chem. Soc., Chem. Commun.* **1992**, *11*, 804−806.
(49) Matias, V. R. F.; Beveridge, T. J. Lipoteichoic Acid Is a Major Component of the Bacillus subtilis Periplasm. *J. Bacteriol.* **2008**, *190* (22), 7414−7418.

DOI: 10.1021/acs.biomac.7b00800
Biomacromolecules XXXX, XXX, XXX−XXX